Development of Doped Hybrid Xerogels as Optical Fibre Sensors for Environmental pH Monitoring

B. Rosales-Reina, N. Whittaker, C. Elosúa, S. Reinoso, T. Sun, K. T. V. Grattan, J. J. Garrido

***Abstract*—A set of optical fibre sensors (OFSs) for pH detection have been prepared by doping hybrid xerogel (XG) matrices with pH indicators for environmental monitoring. The hydrophobic sol-gel siliceous materials were synthesised from propyltriethoxysilane (pTEOS) and tetraethoxysilane (TEOS), and subsequently doped with phenolphthalein, bromophenol blue and cyanidin chloride, resulting in three photonic pH devices (OFS5pTEOSPH, OFS5pTEOSBP and OFS5pTEOSCY). Among them, OFS5pTEOSBP exhibited the best sensing performance, showing a reversible optical response in the pH range from 2 to 6 with an intensity ratio variation from 0.92 to 0.52. The developed sensors exhibit negligible dye leaching, good stability, reproducibility, reversible response, and low hysteresis, with response time from 5 to 190 s depending on the pH. Moreover, their applicability was validated through pH measurements in real soil samples.**

***Index Terms*— Hybrid xerogel, optical fibre sensor, pH indicator, soil pH monitoring.**

I. INTRODUCTION

THE measurement of pH is important today in several applications, such as biochemistry, chemistry, and environmental science [1], [2], [3], and different types of pH sensors have been developed in recent years [4], [5]. The most used device is the specific electrode type [6] which provides high accuracy and sensitivity. However, it is not ideal for all applications and can show fragility, which leads to a degradation of the performance, and requires frequent recalibrations. In this context, OFSs offer many advantages for measuring pH, highlighting their small sensing volume, remote sensing [5], [7], [8], and specially, the fact that they do not need any reference signal as the pH electrodes require [9], [10]: these features make them suitable for many applications to physical and chemical detection [11], [12], [13], [14]. Most optical pH sensors rely on the use of pH colorimetric or fluorometric indicators [15], among them organic pH-sensitive indicators have been widely used in optical pH sensing [16] but they have the disadvantages of the limited stability and leaching. A strategy to reduce leakage of the indicator (which can be inconvenient in some applications) consists of immobilizing the indicator in a sol-gel matrix, becoming one of the most widely used and effective solid matrices for pH sensors [17].

The sol–gel methodology has been broadly adopted for the preparation of sensitive coatings, providing excellent and highly tuneable materials [18]. The process involves hydrolysis and condensation reactions of alkoxide precursors in the presence of water, leading to the formation of silica oligomers within the sol and, subsequently, a gel when the solvent is evaporated [19]. The films prepared with this method are highly stable, optically transparent, and do not swell. In addition, this approach is well-adapted for the deposition of thin films on optical fibres by dip-coating. Through proper tailoring of the material properties, the design of the pore surface chemistry and the porosity can be optimised to minimise dye leaching, important in this and other applications.

This work has been focused on monitoring pH changes in soil, exploiting the positive features of a photonic sensor developed for the purpose. The objectives of the research included: a) characterising XGs, which were doped with the pH indicators phenolphthalein (PH), bromophenol blue (BP) and cyanidin chloride (CY), suitable for a pH range 2 to 7; b) constructing OFSs using the doped hybrid XGs; and c) evaluating their performance towards pH buffer solutions and real soil samples. The pH indicators were selected based on their detection range and solubility in ethanol, and they were used to prepare three different XGs based on the 5pTEOS matrix [20], namely 5pTEOSPH, 5pTEOSBP, and 5pTEOSCY. The inclusion of propylsilane groups into the silica matrix lowers the hydrophilicity and porosity, provides a more flexible matrix structure and reduces the film cracking [21] of the resulting hybrid materials compared to pure silica XGs made from TEOS. These characteristics minimised the leaching of the embedded pH indicators when the sensors were exposed to the measurement medium. The propylsilane molar content was set to 5% because, as demonstrated in a previous work [20], this percentage was found effective in tuning the chemical surface properties of the materials. The three doped hybrid XGs were characterised from the textural and structural viewpoint to unravel their chemical and physical properties, after which they were deposited onto the tip of an optical fibre to develop a set

B. Rosales-Reina, S. Reinoso, and J. J. Garrido are with the Institute for Advanced Materials and Mathematics (INAMAT^2), Departamento de Ciencias, Universidad Pública de Navarra (UPNA), Campus de Arrosadia, Pamplona, 31006 Spain (e-mail: beatriz.rosales@unavarra.es; santiago.reinoso@unavarra.es; j.garrido@unavarra.es).

N. Whittaker, T. Sun and K T. V. Grattan are with School of Science and Technology, City St George's, University of London, London EC1B 0HB, UK (e-mail: Nancy.Whittaker@city.ac.uk, T.Sun@city.ac.uk, K.T.V.Grattan@city.ac.uk).

C. Elosúa is with the Institute of Smart Cities (ISC), Departamento de Electricidad, Electrónica y de Comunicación, Universidad Pública de Navarra (UPNA), Campus de Arrosadia, Pamplona, 31006 Spain (e-mail: cesar.elosua@unavarra.es).

Color versions of one or more of the figures in this article are available online at http://ieeexplore.ieee.org

of sensors working in a reflection architecture. Furthermore, the OFS response in this work can be seen to be self-referenced, using the ratio between intensity peaks, leading to a direct response for which no reference signal is required (as it is for electrode-based sensors). The best performing sensor showed a reversible, repetitive and reproducible behaviour in pH buffers from 2 to 6. Moreover, the potential application for soil pH monitoring was confirmed by real samples in the acidic pH range.

II. Experimental aspect

A. Preparation and characterisation of the doped hybrid xerogel

The three hybrid silica XGs doped with organic guest molecules were synthesised using the sol-gel method [22]. The selected guests were the following three species commonly used as colorimetric pH indicators: disodium 4-[1-(4-oxidophenyl)-3-oxo-2-benzofuran-1-yl]phenolate or phenolphthalein (PH, purity > 99%, from Merck), 3,3′,4,5,7-pentahydroxyflavylium chloride or cyanidin chloride (CY, purity > 96%, from Glenthan Life Sciences, Planegg, Germany), and 3′,3″,5′,5″-tetrabromophenolsulfonephthalein or bromophenol blue (BP, purity > 95%, from Merck). TEOS (purity > 99%) and pTEOS (purity > 97%) were purchased from Sigma Aldrich. The (TEOS+pTEOS):EtOH:H_2O molar ratio used for the synthesis of these materials was 1.00:4.75:5.50, where the TEOS and pTEOS precursor mixture all contained, a fixed 0.95:0.05 molar ratio, to generate a hybrid 5pTEOS matrix. The doped XGs obtained following this procedure were labelled as 5pTEOSPH, 5pTEOSCY, and 5pTEOSBP for phenolphthalein, cyanidin chloride, and bromophenol blue respectively.

The colorimetric indicators were introduced into the synthetic medium as the ethanolic fraction as it follows:70 mM ethanolic solutions of the pH indicators were added dropwise to the TEOS and pTEOS mixture under continuous stirring, resulting in a final concentration of 31.50 mM in the alcoholic media. Milli-Q grade water was subsequently added dropwise, and the final pH was then adjusted to 2.00 using a 0.10 M HCl(aq) solution added with a Pasteur pipette. The vessels containing the resulting sols were sealed with paraFILM^{TM} and placed in an oven at 60 °C (Thermo Electron LED T6, from Thermo Scientific, Massachusetts, USA) to promote gelation. Once the alcogels were formed, the vessels were kept closed under ambient conditions for one week and opened afterwards to allow the solvent evaporation, leading to obtaining the final materials as monoliths.

B Optical set-up

To prepare the OFS from the XGs described above, optical fibre pigtails with inner and outer diameters of 200 and 225 µm, respectively (FT200UMT, Thorlabs) were used. The active sensing layer was coated onto the optical fibre planar cut end using a process involving 1 immersion (immersion/extraction speed rate of 150/10 mm min^{-1}) into the different, freshly prepared solutions (gelation time equal to 0), enabling the creation of three different probes (with a different indicator each), labelled OFS5pTEOSPH (phenolphthalein), OFS5pTEOSBP (bromophenol blue) and OFS5pTEOSCY (cyanidin blue). As it is reported in previous works about sensors fabricated with this type of XGs, the coating thickness is expected to be lower than 400nm [20].

An OceanInsight HDX spectrometer together with a DH-2000-SDUV-TTLO halogen lamp from Mikropack , were used to characterise the probes (see Fig. 1). These devices were connected by a 200 µm bifurcated fibre for UV-vis (UV-vis 50:50 Y coupler, from OceanOptics). The integration time selected was 500 ms, the scans average and the boxcar width were set at 3, the spectra were saved every 5 s, and the sensors were kept in each buffer solution for 20 min.

The response was characterised by the intensity ratio between the two most intense peaks (I_1 and I_2) from the reflected signal spectra. This measuring method offered the advantage of being faster and simple because it does not need to first compute the absorbance and then interpret the spectra.

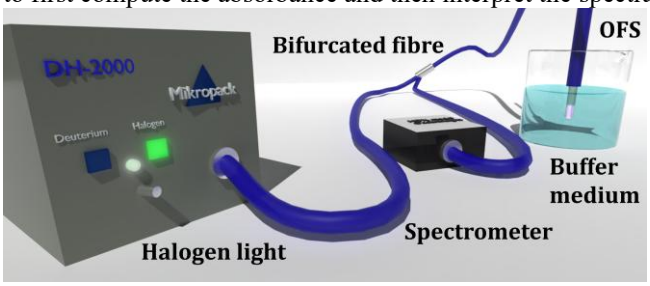

Fig. 1. Experimental set-up to register the sensor response.

C. Characterisation

The physical properties of the three different pH indicators (PH, BP, and CY) used to dope the hybrid XG matrix 5pTEOS are summarised in Table AI in the Appendix. The resulting doped XG materials (5pTEOSPH, 5pTEOSBP, and 5pTEOSCY) were characterised and compared to the TEOS and 5pTEOS reference XGs in terms of: a) powder X-ray diffraction (PXRD); b) Fourier Transform infrared spectroscopy (FT-IR); c) thermogravimetric analysis and differential scanning calorimetry (TGA/DSC) and d) adsorption-desorption isotherms using N_2 (−196 °C), CO_2 (0 °C), and water vapour (25 °C). A detailed description of these techniques, the parameters used in these characterisation experiments, and the interpretation of the diffraction patterns, FT-IR spectra and TGA-DSC analyses is available in the Appendix. All this characterisation was found useful to verify that the pH indicators were integrated into the XG matrix, and that their structural and thermal properties were not negatively affected.

Fig. 2 shows the N_2 and CO_2 the adsorption-desorption isotherms, while the derived textural parameters are collected in Table I. All the isotherms are of type I(b) based on the IUPAC classification [23], which corresponds to mainly microporous materials with a narrow pore size distribution (PSD), that are favourable for the construction of the OFSs.

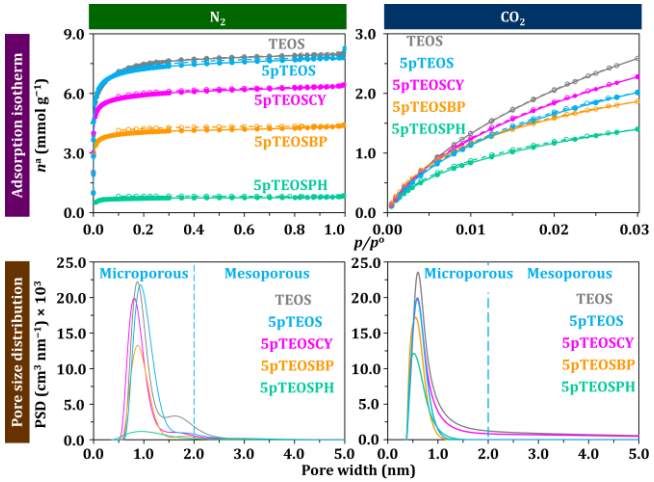

Fig. 2. Adsorption-desorption isotherms registered with N_2 (−196 °C) and CO_2 (0 °C) for the reference TEOS and 5pTEOS materials and for the xerogels doped with pH indicators, along with pore size distributions (lines-markers: adsorption, continuous-filled; desorption, dashed-empty).

TABLE I

TEXTURAL PARAMETERS OF THE TEOS AND 5PTEOS REFERENCE MATERIALS AND THE XEROGELS DOPED WITH PH INDICATORS AS DERIVED FROM THE N_2 AND CO_2 ADSORPTION-DESORPTION ISOTHERMS.

	TEOS	5pTEOS	5pTEOSPH	5pTEOSBP	5pTEOSCY
a_{BET} (N_2) (m^2 g^{-1})	697	607	61	349	506
a_{DR} (CO_2) (m^2 g^{-1})	510	444	282	384	501
V_{micro}[a] (N_2) (cm^3 g^{-1})	0.28	0.25	0.03	0.14	0.21
V_{micro}[b] (CO_2) (cm^3 g^{-1})	0.19	0.19	0.12	0.16	0.21
V_{meso}[c] (N_2) (cm^3 g^{-1})	0.12	0.01	NEGL	NEGL	NEGL
V_T[d] (N_2) (cm^3 g^{-1})	0.41	0.27	0.03	0.15	0.22
E_c[e] (N_2) (kJ mol^{-1})	15.7	18.7	13.6	20.5	19.3
E_c[e] (CO_2) (kJ mol^{-1})	19.9	19.6	20.8	20.8	19.4

[a] Calculated from the isotherms at p/po = 0.30: [b] Micropore volume obtained from the DR model (see the Appendix); [c] Calculated as $V_{meso}=V_T-V_{macro}-V_{micro.}$; [d] Total pore volume obtained from the isotherms at p/po = 0.95; [e] Characteristic energy obtained from DR model (see the Appendix).

The embedding of the pH indicator into the 5pTEOS XG matrix resulted in a decrease in the a_{BET}, which follows the order: 5pTEOSCY > 5pTEOSBP > 5pTEOSPH. Notably, 5pTEOSPH barely adsorbs N_2 and exhibited the narrowest pore distribution according to the CO_2 adsorption-desorption isotherm, thus being a mainly ultramicroporous material. This suggests an active diffusion process, as the pore volumes are extremely narrow, and the kinetic energy of the N_2 molecule at −196 °C is not enough to access the materials surface effectively [24]. The characteristic energy increased as the a_{BET} decreased, the order being the reverse of that mentioned above for a_{BET}. Considering all the textural parameters and the adsorption-desorption isotherms, the materials were found to be mostly microporous. This feature should not constitute any drawback for their use in the construction of pH sensors, since the aim for the XG coating is to interact reversibly with the medium.

The final sensors developed were to be used in aqueous media, so that a labile interaction with water was required. This characteristic was explored through adsorption-desorption isotherms of water vapour performed at 25 °C, which are shown in Fig. 3.

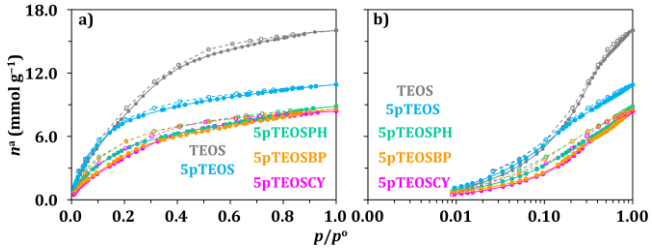

Fig 3. a) Water vapour adsorption-desorption isotherm at 25 °C and b) semilog representation for the references (TEOS and 5pTEOS) and the doped hybrid xerogels (5pTEOSPH, 5pTEOSBP, and 5pTEOSCY).

The doped hybrid XGs all exhibited very similar behaviour, which differs from those of the TEOS and 5pTEOS references in their adsorption quantities at low pressure values. The isotherms from the doped hybrid XGs could be classified as type I(b), with nearly negligible hysteresis loops. According to the textural parameters in Table II, the inclusion of propylsilane groups (5pTEOS) decreased a_{BET} and the mesoporous volume (V_{meso}) in comparison with TEOS, the former parameter being further reduced upon inclusion of the pH indicators. Among the doped hybrid XG materials, slight differences were observed in a_{BET}, as well as in the microporous (V_{micro}) and mesoporous (V_{meso}) volumes, showing larger hysteresis loops than the reference materials. The semilogarithmic graph in Fig. 3b displays in detail the microporous region, highlighting the similarities between the three doped hybrid XGs and the differences in the mesoporous region for the reference materials.

TABLE II

TEXTURAL PARAMETERS OF THE REFERENCE MATERIALS TEOS AND 5PTEOS AND THE XEROGELS DOPED WITH PH INDICATORS AS DERIVED FROM THE ADSORPTION-DESORPTION ISOTHERMS WITH WATER VAPOUR.

	TEOS	5pTEOS	5pTEOSPH	5pTEOSBP	5pTEOSCY
q_m[a] (mmol g^{-1})	9.43	6.87	4.81	4.77	4.62
a_{BET} (m^2 g^{-1})	710	517	362	359	348
V_{micro}[b] (cm^3 g^{-1})	0.18	0.14	0.10	0.09	0.09
V_{meso}[c] (cm^3 g^{-1})	0.10	0.04	0.05	0.05	0.05
V_{total}[d] (cm^3 g^{-1})	0.29	0.19	0.16	0.14	0.15
E_c[e] (kJ mol^{-1})	7.64	7.94	8.63	8.26	7.83

[a] Monolayer capacity obtained by the BET (see the Appendix); [b] Micropore volume obtained from the isotherms at p/p° = 0.30; [c] Mesopore volume obtained from the isotherms (0.8 < p/p° < 0.95); [d] Total pore volume obtained from the isotherms at p/p° = 0.95;[e] Characteristic energy obtained from DR model (see the Appendix).

The adsorption-desorption isotherms with water vapour at 25 °C demonstrate that the studied doped hybrid XGs could be used in aqueous solution. No condensation occurred at $p/p^o = 1$ and the adsorption-desorption process was reversible, as the starting and the ending points of the adsorption and desorption branches matched in all cases. Furthermore, the incorporation of propyl groups enhanced the hydrophobic character of the

materials surface and could be leading to a reversible sensor response.

D. Optical fibre sensor characterisation for different pH buffers

The doped hybrid XGs were used to prepare the sensors OFS5pTEOSPH, OFS5pTEOSBP, and OFS5pTEOSCY. Their performance was evaluated in the pH scale from 2 to 6 to preserve the integrity of the doped hybrid XG coating. The results are displayed in Fig. 4.

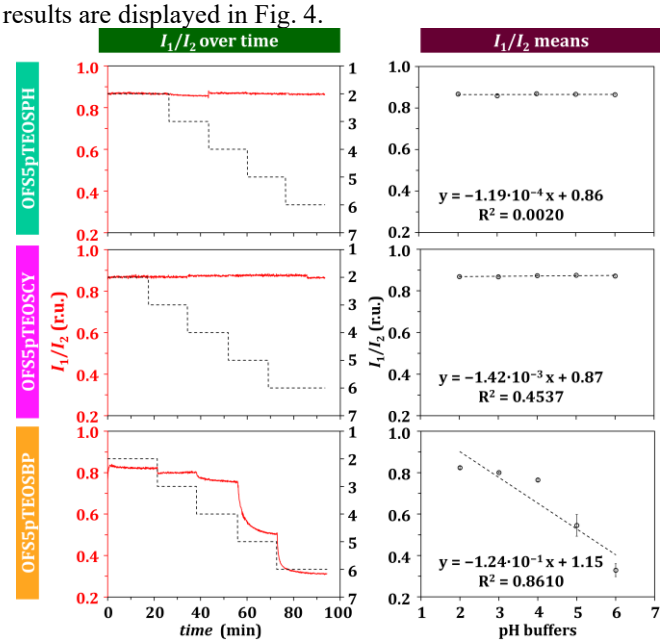

Fig. 4. Left column: time response in terms of the intensity ratio of sensor (red line) for different pH steps (dashed line); right column: average value of the intensity ratio for different pH buffers.

The OFS5pTEOSPH probe showed negligible changes because the XG colour transitions from colourless to yellowish at pH = 6, and then to pink at pH = 12, these pH values lying out of the working range. In the case of OFS5pTEOSCY, the XG colour goes from red in strongly acidic pH to purple at pH = 4, and then to blue at pH = 6, but the CY molecules were very sensitive to the storage temperature, limiting the sensor performance. Finally, OFS5pTEOSBP showed the highest sensitivity, with the ratio I_1/I_2 (R^2 = 0.8610) varying from 0.90 at pH = 2 to 0.52 at pH = 6, the colour changing from orange to blue when the pH went from 2 to 4 (see Fig. A1). Therefore, OFS5pTEOSBP was selected for the subsequent tests.

Fig. 5 shows the spectra recorded for OFS5pTEOSBP after being immersed for 10 minutes in different pH buffer solutions. It can be observed how the intensities of the two monitored I_1 and I_2 peaks vary with the pH.

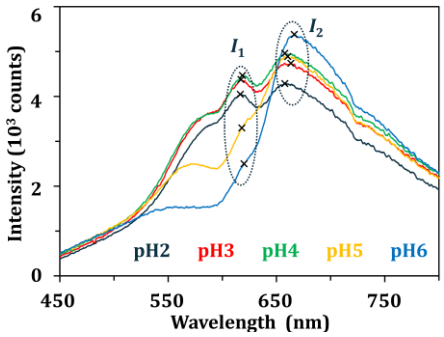

Fig. 5. Variations in the peaks (I_1 and I_2) intensity for OFS5pTEOSBP.

E. Optical fibre sensor reproducibility and repeatability for different pH buffers

To evaluate the reproducibility, a second probe was prepared, so the two sensors were labelled as OFS5pTEOSBP1 (original) and 2 (replica). Applying a sequence of decreasing and increasing pH values over two consecutive cycles using five different pH buffer solutions (pH = 2, 3, 4, 5, and 6) allowed also the repeatability and the hysteresis of these probes to be evaluated. Fig. 6 displays both the real time value of the intensity ratios and the corresponding calibrations. Each sequence of decreasing / increasing pH values was repeated twice to confirm repeatability: the ratio values for each pH were averaged to obtain the calibration lines, using their standard deviation as error bars. The response is reversible (with a low hysteresis) and, overall, both sensors follow a similar trend. To evaluate the hysteresis between the increasing and decreasing branches of the pH value, the area enclosed between the branches was calculated. The values obtained (listed in Table AIV), were around 0.1 in both cases, being somewhat smaller for OFS5pTEOSBP1. The response time (Figure A5a) for both sensors is similar: the shortest times were obtained at pH = 3 (7 and 5 s for probes 1 and 2, respectively), whereas the longest responses were observed at pH = 6 for the sensor 1 (187 s) and at pH = 5 on the decreasing branch of the pH scale for the sensor 2 (148 s).

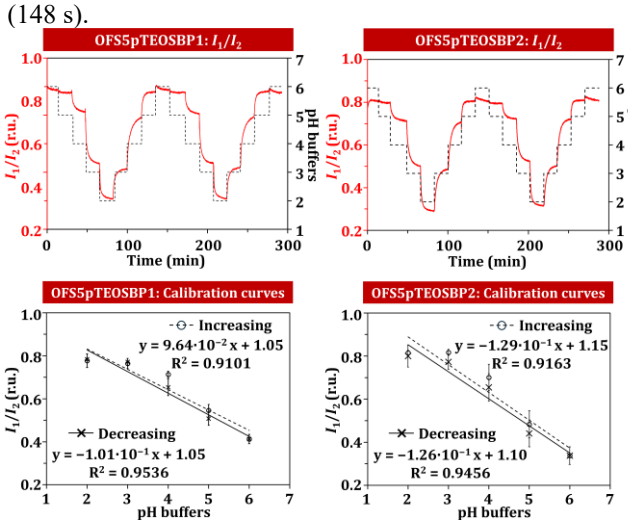

Fig. 6. Top row: intensity ratios over time for different pH values (2, 3, 4, 5, and 6); bottom row: the corresponding calibrations lines for decreasing and increasing pH values.

The value obtained for pH = 2 in these tests, deviates significantly from the trend for both sensors; therefore, a new reproducibility test with OFS5pTEOSBP1 was carried out in the pH range from 3 to 6, but applying pH variation steps of 0.5, units instead of 1.0 (Fig. 7). The result obtained showed higher R^2 values (0.9661 and 0.9764 respectively).

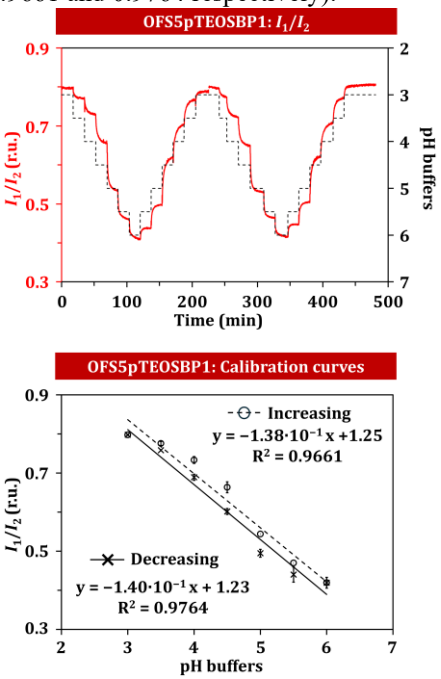

Fig. 7. Intensity ratio of OFS5pTEOSBP1 for a sequence of decreasing and increasing pH values and calibration approaches to show long-term stability.

The dynamic range obtained in the reproducibility and repeatability experiments have similar values (in Fig. 7 the dynamic range was from 0.80 to 0.42 while in Fig. 6 was from 0.81 to 0.32). These slight variations were observed at the higher limits of the working range, in which the response was less linear. For this sensor, the shortest response time (Figure A5b) was obtained at pH = 3 (5 s), while the longest one was observed at pH = 4.5 (150 s) on the increasing branch of the pH scale. The hysteresis loop calculated was similar to that of the previous test (HL = 0.10), as shown in Table AIV.

F. pH monitoring of real soil samples by OFS5pTEOSBP1

To verify the performance in a practical environmental test, an evaluation was conducted using real soil samples (the properties of which can be found in Table AV) with modified pH. To achieve this modification, their moisture content was set at 50% by firstly drying the samples overnight at 200 °C in an oven, and then, adding an amount of buffer solution equal to half of the dried sample mass. The resulting pH was verified by a litmus paper test, before performing the evaluation. The response of OFS5pTEOSBP1 was characterised by a sequence of samples with increasing-decreasing pH (see Fig. 8). The sensitivity obtained for the soil test was slightly lower than that for the pH buffers (from 0.66 to 0.38), but the same behaviour trend was observed: when the pH increases the intensity ratio decreases and vice versa, this trend being reversible, repetitive and with a low hysteresis. It is also noticeable that the different OFS5pTEOSBP1 tests were performed during different days, confirming the stability of the probes over time.

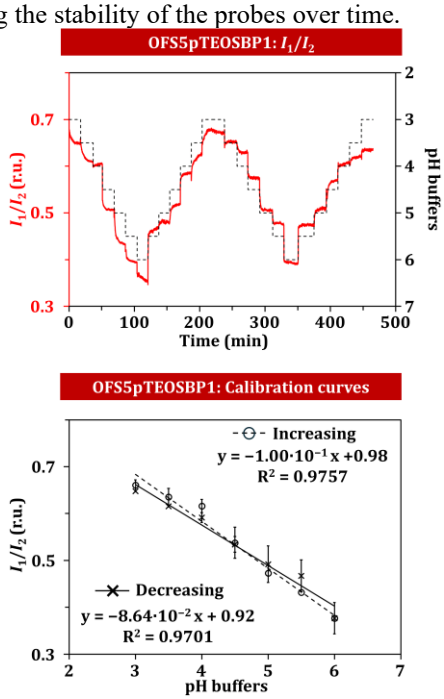

Fig. 8. Intensity ratios of OFS5pTEOSBP1 when immersed in soil samples with different pH values and the corresponding calibration approaches.

The response time values registered, (see Fig AVb) differ slightly from those obtained with the same sensor when exposed to the buffer solutions. This may be due to the fact that these measurements were carried out in a different medium, where the signal stability could have been affected. On the other hand, the hysteresis obtained was the lowest (0.0001, Table AIV), which indicates the reversibility of the measurements.

Table III provides a bibliographic summary of the characteristics of different sensors used to measure buffer solutions. According to this summary the sensor presented in this work shows a higher measurement pH range than those found in the literature.

TABLE III

COMPARISON OF THE OFS5PTEOSBP PERFORMANCE TO THOSE OF OTHER SENSORS WITH DIFFERENT SENSING MATERIALS AND CONFIGURATIONS.

Configuration	Material	pH range	Medium	Ref
ΔElectrical Resistance	SWNTs	5-9	Buffers	[25]
Colorimetric	TEOS, CR, ChR and BR	2-13	Buffers	[26]
Optical transmission	PEI/PAA	5.92–9.23	Buffers	[12]
	Phenol red in a silica	1-10	Buffers	[13]
	Dye contained in an H^+	7.0-7.4	Blood	[4]
	PR-MSNE	1-10	Buffers	[11]
Optical Interferometer	SA/PEI	2-11	Buffer	[5]
Optical reflection	FBG	5-7	Buffers	[27]
	mPOFBG	5-7	Buffers	[27]
	5pTEOSBP	2-6	Buffers / Soil	This work

CR: CRESOL RED, CHR: CHLOROPHENO RED, BR: BROMPHENOL REDSWNTS: SINGLE-WALLED CARBON NANOTUBES, PEI: POLYETHYLENEIMINE, PAA: POLY(ACRYLIC ACID), SA: SELF-ASSEMBLED SODIUM ALGINATE, PR-MSN: PHENOL RED DYE FUNCTIONALIZED MESOPOROUS SILICA NANO-STRCTURES/NANO TUBES FBG: FIBER BRAGG GRATTING, MPOFBG: MICROSTRUCTURED POLYMER OPTICAL FIBER BRAGG GRATING.

CONCLUSION

The research carried out has shown that the hybrid silica xerogel containing 5% propyl-substituted silica can be successfully employed as robust host matrix for pH indicators, enabling the construction of optical fibre sensors with enhanced stability and repeatability. Of the three doped xerogels prepared, the bromophenol blue (BP) based material (5pTEOSBP) exhibited the most reliable and sensitive optical response, characterised by a reversible response in the intensity ratio between the monitored spectral peaks in the pH interval from 3 to 6. The sensing mechanism, based on self-referenced optical measurements, avoids using external reference signals, leading to an improved reproducibility. Moreover, negligible leaching, low hysteresis values, and response times as short as a few seconds under acidic conditions confirmed the robustness of the sensing layer. It is remarkable that the sensors performance was preserved when applied to real soil samples, confirming its suitability for environmental pH monitoring.

Nonetheless, the working range of the developed sensors remains constrained by the hydrolytic degradation of the xerogel coating under alkaline media, limiting reliable operation above pH 6.

In summary, this study presents a proof of concept for the use of doped hybrid xerogels as optically responsive coatings, paving the way for advanced pH sensing strategies. Future developments should focus on extending the long-term chemical stability of the hybrid network, integrating additional chromophore systems to broaden detection ranges, and adapting the approach for multiplexed or distributed sensing platforms, particularly in environmental and agriculture monitoring applications.

APPENDIX

The appendix includes the materials characterisation additional data and graphs, as well as the colour change of the monolith in the pH working range.

ACKNOWLEDGMENT

B. R.-R. thanks the financial support from the Ministry of Science e Innovation, Government of Spain (PID2020-113558RB-C42 and PID2022-137437OB-I00), and a mobility grant from Universidad Pública de Navarra. N. W. would like to thank the Industrial PhD Partnership scheme part of the Future Aviation Security.
Solutions (FASS) programme - a joint Department for Transport and Home Office initiative - with support from Smiths Detection-Watford Limited is gratefully appreciated.

REFERENCES

[1] J. Heikenfeld, A. Jajack, B. Feldman, S. W. Granger, S. Gaitonde, G. Begtrup, B. A. Katchman, "Accessing analytes in biofluids for peripheral biochemical monitoring," *Nat. Biotechnol*, vol. 37, pp. 407–419, Feb. 2019, doi: 10.1038/s41587-019-0040-3.

[2] J. Saiz-Poseu, J. Mancebo-Aracil, F. Nador, F. Busqué, D. Ruiz-Molina, "The chemistry behind catechol-based adhesion," *Angew. Chem. Int. Ed.,* vol. 58, pp. 696–714, Jan. 2019, doi: 10.1002/anie.201801063.

[3] R. Kishor, D. Purchase, G. Dattatraya, R. Ganesh, L. F. Romanholo, M. Bilal, R. Chandra, R. Naresh, "Ecotoxicological and health concerns of persistent coloring pollutants of textile industry wastewater and treatment approaches for environmental safety," *J. Environ. Chem. Eng.,* vol. 9, Art. no. 105012, Apr. 2021, doi: 10.1016/j.jece.2020.105012.

[4] M. T. Ghoneim, A. Nguyen, N. Dereje, J. Huang, P. J. Murzynowski, C. Dagdeviren, "Recent progress in electrochemical pH-sensing materials and configurations for biomedical applications," *Chem. Rev.,* vol. 119, pp. 5248–5297. Mar. 2019, doi: 10.1021/acs.chemrev.8b00655.

[5] A. Steinegger, O. S. Wolfbeis, S. M. Borisov, "Optical sensing and imaging of pH values: spectroscopies, materials, and applications," *Chem. Rev.*, vol. 120, pp. 12357–12489, Nov. 2020, doi: 10.1021/acs.chemrev.0c00451.

[6] H. Yin, Y. Cao, B. Marelli, X. Zeng, A. J. Mason, C. Cao, "Soil sensors and plant wearables for smart and precision agriculture," *Adv. Mat.*, vol. 33, Art. no. 2007764, May 2021, doi: 10.1002/adma.202007764.

[7] F. Ofridam, M. Tarhini, N. Lebaz, É. Gagnière, D. Mangin, A. Elaissari. "pH-sensitive polymers: classification and some fine potential applications," *Polym. Adv. Technol.*, vol. 32, pp. 1455–1484, Apr. 2021, doi: 10.1002/pat.5230.

[8] M. Adeel, M. M. Rahman, I. Caligiuri, V. Canzonieri, F. Rizzolio, S. Daniele, "Recent advances of electrochemical and optical enzyme-free glucose sensors operating at physiological conditions," *Biosens. Bioelectron.*, vol. 165, Art. no. 112331, May 2020, doi: 10.1016/j.bios.2020.112331.

[9] W.-H. Chen, W. D. N. Dillon, E. A. Armstrong, S. C. Moratti, C. M. McGraw, "Self-referencing optical fiber pH sensor for marine microenvironments," *Talanta* vol. 225, Art. no. 121969, Apr. 2021, doi: 10.1016/j.talanta.2020.121969.

[10] S.-J. Choi, Y.-C. Kim, M. Song, J.-K. Pan, "A self-referencing intensity-based fiber optic sensor with multipoint sensing characteristics," *Sensors*, vol. 14, pp. 12803–12815, Jul. 2014, doi: 10.3390/s140712803.

[11] W. Liu, C. Liu, J. Wang, J. Lv, Y. Lv. L. Yang, N. An, Z. Yi, Q. Liu, C. Hu, P. K. Chu, "Surface plasmon resonance sensor composed of microstructured optical fibers for monitoring of external and internal environments in biological and environmental sensing," *Results Phys.* vol. 47, Art. no. 106365, Apr. 2023, doi: 10.1016/j.rinp.2023.106365.

[12] J. M. Pereira, J. P. Mendes, B. Dias, J. M. M. M. de Almeida, L. C. C. Coelho, "Optical pH sensor based on a long-period fiber grating coated with a polymeric layer-by-layer electrostatic self-assembled nanofilm," *Sensors*, vol. 24, Art. no. 1662, Mar. 2024, doi: 10.3390/s24051662.

[13] B. R. Gomes, R. Araújo, T. Sousa, R. B. Figueira, "Sol-gel coating membranes for optical fiber sensors for concrete structure monitoring," *Coatings,* vol. 11, Art. no. 1245, Oct. 2021, doi: 10.3390/coatings11101245.

[14] R. Cao, H. Ding, K.-J. Kim, Z. Peng, J. Wu, J. T. Culp, P. R. Ohodnicki, E. Beckmand, K. P. Chen, "Metal-organic framework functionalized polymer coating for fiber optical methane sensors," *Sens. Actuators B*, vol 324, Art. no. 128627, Dec. 2020, doi: 10.1016/j.snb.2020.128627.

[15] X.-d. Wang, O. S. Wolfbeis, "Fiber-optic chemical sensors and biosensors (2015-2019)," *Anal. Chem*., vol. 92, pp. 397–430, Jan. 2020, doi: 10.1021/acs.analchem.9b04708.

[16] S. Islam, H. Bakhtiar, S. Naseem, M. S. B. Abd-Aziz, N. Bidin, S. Riaz, J. Ali, "Surface functionality and optical properties impact of phenol red dye on mesoporous silica matrix for fiber optic pH sensing," *Sens. Actuators, A*, vol. 276, pp. 267–277, Jun. 2018, doi: 10.1016/j.sna.2018.04.027.

[17] F. Lu, R. Wright, P. Lu, P. C. Cvetic, P. R. Ohodnicki, "Distributed fiber optic pH sensors using sol-gel silica based sensitive materials," *Sens Actuators, B*, vol. 340, Art. no. 129853, Aug. 2021, doi: 10.1016/j.snb.2021.129853.

[18] B. Schyrr, S. Pasche, E. Scolan, R. Ischer, D. Ferrario, J.-A. Porchet, G. Voirin, "Development of a polymer optical fiber pH sensor for on-body monitoring application," *Sens. Actuators, B*, vol. 194, pp. 238–248, Apr. 2014, doi: 10.1016/j.snb.2013.12.032.

[19] G. Cruz-Quesada, M. Espinal-Viguri, M. V. López-Ramón, J. J. Garrido, "Novel organochlorinated xerogels: from microporous materials to ordered domains," *Polymers*, vol. 13¸ Art. no. 1415, Apr. 2021, doi: 10.3390/polym13091415.

[20] B. Rosales-Reina, D. López-Torres, G. Cruz-Quesada, M. Espinal-Viguri, C. Elosúa, S. Reinoso, J. J. Garrido, "Tuning the sensitivity of photonic sensors toward alkanes through the textural properties of hybrid xerogel coating," *Adv. Funct. Mater*., vol. 35, Art. no. 2413871, Jan. 2025, doi: 10.1002/adfm.202413871.

[21] M. M. Collinson, "Recent trends in analytical applications of organically modified silicate materials," *TrAc. Trends Anal. Chem*., vol. 21, pp. 31–39, Jan. 2002, doi: 10.1016/S0165-9936(01)00125-X.

[22] G. Cruz-Quesada, M. Espinal-Viguri, M. V. López-Ramón, J. J. Garrido "Novel silica hybrid xerogels prepared by co-condensation of TEOS and ClPhTEOS: a chemical and morphological study," *Gels*, vol. 8, Art. no. 677, Oct. 2022, doi: 10.3390/gels8100677.

[23] M. Thommes, K. Kaneko, A. V. Neimark, J. P. Oliver, F. Rodriguez-Reinoso, J. Rouquerol, K. S. W. Sing, "Physisorption of gases, with special reference to the evaluation of surface area and pore size distribution (IUPAC Technical Report)," *Pure Appl. Chem*., vol. 87, pp. 1051–1069, Jul. 2015, doi: 10.1515/pac-2014-1117.

[24] F. d'Acapito, "X-ray absorption spectroscopy studies on materials obtained by the sol-gel route," in *Handbook of Sol-Gel Science and Technology: Processing, Characterization and Applications*, 2nd ed., L. Klein, M. Aparicio, A. Jitianu, Eds. Cham, Switzerland: Springer, 2018, pp. 1231-1255.

[25] P. Li, C. M. Martin, K. K. Yeung, W. Xue, "Dielectrophoresis aligned single-walled carbon nanotubes as pH sensors," *Biosensors*, vol. 1, pp. 23–25, Jan. 2011, doi: 10.3390/bios1010023.

[26] V. Bhardwaj, A.K. Pathak, K. Singh, "No-core fiber-based highly sensitive optical fiber pH sensor," *J. Biomed. Opt*., vol 22, Art. no. 057001, May 2017, doi: 10.1117/1.JBO.22.5.057001.

[27] J. Janting, J.K.M. Pedersen, G. Woyessa, K. Nielsen, O. Bang, "Small and robust all-polymer fiber Bragg grating based pH sensor," *J. Light. Technol*., vol. 37, pp. 4480–4486, Sept. 2019, doi: 10.1109/JLT.2019.2902638.